Flow Curvature Effect on Dynamic Behaviour of a Novel Vertical Axis Tidal Current Turbine: Numerical and Experimental Analysis

Conference Paper · January 2005

DOI: 10.1115/OMAE2005-67193

CITATIONS
6

READS
40

5 authors, including:

Domenico Coiro
University of Naples Federico II
58 PUBLICATIONS **208** CITATIONS
SEE PROFILE

Fabrizio Nicolosi
University of Naples Federico II
60 PUBLICATIONS **236** CITATIONS
SEE PROFILE

Agostino De Marco
University of Naples Federico II
40 PUBLICATIONS **118** CITATIONS
SEE PROFILE

Proceedings of OMAE2005:
24th International Conference on
Offshore Mechanics and Arctic Engineering
Halkidiki, Greece 12-17 June 2005

OMAE2005-67193

FLOW CURVATURE EFFECTS ON DYNAMIC BEHAVIOUR OF A NOVEL VERTICAL AXIS TIDAL CURRENT TURBINE: NUMERICAL AND EXPERIMENTAL ANALYSIS

Domenico Coiro
University of Naples "Federico II"

Fabrizio Nicolosi
University of Naples "Federico II"

Agostino De Marco
University of Naples "Federico II"

Stefano Melone
University of Naples "Federico II"

Francesco Montella
University of Naples "Federico II"

ABSTRACT

This paper presents a summary of the work done by the authors regarding the design, construction and test of vertical axis hydro turbines to exploit tidal currents. Double Multiple Streamtube (DMS) model and Vortex model have been used to predict turbines performances either with fixed blades or with self-acting variable pitch blades. Within the DMS model, VAWT and VAWT_dyn codes have been developed to analyze steady and dynamic performances; within Vortex model, VAT-VOR3D code has been developed. Theoretical analysis and numerical predicted performances have been compared and validated with experimental test results on both model and real scale turbines. A comparison between DMS and Vortex model results has been presented. Moreover, the recent activities in terms of numerical investigations on the flow curvature effects are presented.

Keywords: Vertical-Axis-Hydro-Turbine; Variable Pitch; Curved Airfoil; Flow Curvature; Tidal Energy.

INTRODUCTION

Marine current energy is a type of renewable energy resources that has been less exploited respect to wind energy. Only in the last few years, some countries have devoted funds to the researches aimed to develop tidal current power stations. The vertical axis turbines could present significant advantages for tidal current exploitation, because they are simple to built and reliable in working conditions. At beginning of the studies, vertical axis wind turbines were taken as models for hydro-turbines, making use of fixed blades; they had good performances when the blade solidity was low and working speed was high. For this reason, the first hydro-turbines were impossible to start. A variable-pitch blades system can be a solution to this problem. So, some prototypes with different kind of this system have been developed around the world: the *KOBOLD* turbine in the Strait of Messina, Italy (Coiro and Nicolosi, 1998), the cycloidal turbine in Guanshan, China (Zhang, 2004), the moment-control turbine in Edinburgh University, UK (Salter, 2001), and the mass-stabilized system turbine by Kirke and Lazauskas (1993) in Inman Valley, South Australia. The methods to calculate the hydrodynamic performances of the vertical axis turbines come from the wind turbines: Templin (1970's) developed the Single-Disk Single-Tube model and then Strickland put forward the Single-Disk Multi-Tube model. Paraschivoiu (1980's) introduced the Double-Disk Multi-Tube model (DMS). The VAWT and VAWT_DYN computer codes, based on this theory, have been developed to predict the steady and dynamic performances of a cycloturbine with fixed or self-acting variable pitch straight-blades. Numerical results have been compared with two sets of experimental data: one set is obtained from wind tunnel test on scaled model and another set is relative to field data of the KOBOLD prototype. To overcome the limits of the DMS model, a 3D vortex method has been used to analyze the performances when solidity is high and comparison with the DMS codes will be presented. Furthermore detailed analysis of flow curvature effect has been performed using panel method technique and the effect of this on the optimal airfoil shape will be discussed.

NUMERICAL INVESTIGATIONS: DOUBLE MULTIPLE STREAMTUBE MODEL

In order to analyse the flow field around a vertical axis turbine, the Double Multiple Streamtube (DMS) (Paraschivoiu, 2002) model has been used. Such model assumes that the flow through the rotor can be modelled by examining the flow through more streamtubes and the flow disturbance, produced by the rotor, is determined by equating the aerodynamic forces on the turbine rotor to the time rate of change in momentum through the rotor. In the DMS model the flow velocities vary in both the upwind and downwind regions of the streamtube as well as varying from streamtube to streamtube. As shown in Fig. 1, the rotor is modelled as a series of elementary streamtubes and each streamtube is modelled with two actuator disks in series. Across the actuator disk the pressure drops and this drop is equivalent to the stream wise force dF on the

actuator disk divided by the actuator disk area dA. θ is the blade angular position.

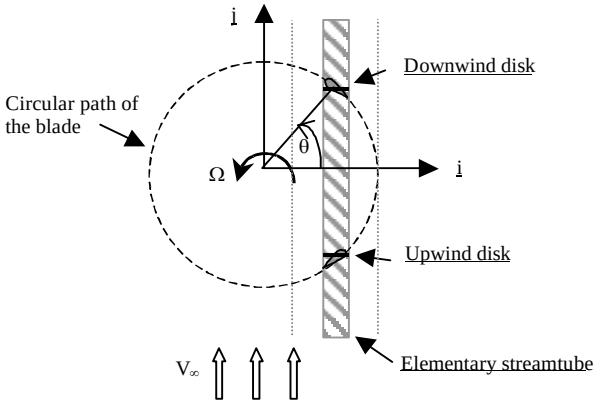

Fig. 1 - Double Multiple Streamtube model

The elementary force dF_u and dF_d, respectively on the upwind (u) and downwind (d) disk, given by the momentum principle, are

$$dF_u = 2\rho a_u (1 - a_u) V_\infty^2 dA_u \quad (1)$$

$$dF_d = 2\rho (1 - a_d)(a_d - 2a_u) V_\infty^2 dA_u \quad (2)$$

where a_u and a_d are the upwind and downwind interference factors defined as

$$a_u = \frac{V_\infty - V_u}{V_\infty} \qquad a_d = \frac{V_\infty - V_d}{V_\infty} \quad (3)$$

V_u and V_d are the velocity on the upwind and downwind actuator disk. The elementary forces dF on the actuator disks may be calculated with the Blade Element Theory. The mathematical problem can be reduced to the calculation of a_u and a_d and, because of non linearity of the equations, the problem must be resolved iteratively. If rotor blades have a fixed pitch angle or an assigned pitch variation, the mathematical model is reduced, for each elementary streamtube, to an equation for the momentum balance for the upwind actuator disk and an equation for the momentum balance for the downwind actuator disk. If rotor blades have a self-acting variable pitch angle (Kentfield, 1983; Lazauskas, 1992; Kirke and Lazauskas, 1993), it is also necessary another equation for each actuator disk: the hinge moment equilibrium. In this case, in fact, the blade is partially free to pitch under the action of the aerodynamic and inertial forces so as to reduce the angle of attack and, hence, the tendency of the blade to stall. Allowed angular swinging of the blade is limited by the presence of two blocks. In this way the mathematical model is represented by two system of equations, each constituted of two equations: momentum balance and hinge moment equilibrium. Instantaneous torque, M, and power, P, produced by the blade are given by the moment equilibrium around turbine axis of the radial and tangential forces. To obtain the mean torque and mechanical power produced by N_b blades in a revolution it is necessary to average the instantaneous values (Montella and Melone, 2003; Coiro, Nicolosi, De Marco, Melone, and Montella, 2004). To simulate dynamic performances of a fixed blades turbine, we have to resolve only the equation of the moment equilibrium around turbine axis, Eq. (5). For a floating blades turbine, we have to add the N_b equations of the moment equilibrium for the N_b blades around their hinge axis, Eq. (6).

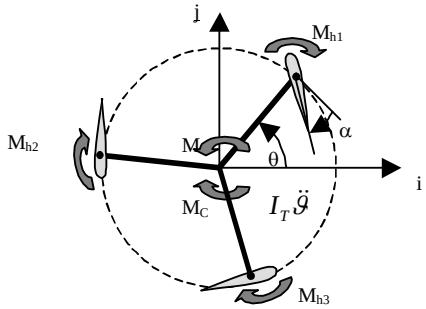

Fig. 2 - Torques on a floating blades turbine

$$I_T \ddot{\vartheta} = \sum_{i=1}^{N_b} M_i - M_C \quad (5)$$

$$I_P (\ddot{\alpha}_1 - \ddot{\vartheta}) = M_{h1}$$
$$I_P (\ddot{\alpha}_2 - \ddot{\vartheta}) = M_{h2} \quad (6)$$
$$I_P (\ddot{\alpha}_3 - \ddot{\vartheta}) = M_{h3}$$
$$\ldots\ldots\ldots$$
$$I_P (\ddot{\alpha}_n - \ddot{\vartheta}) = M_{hn}$$

I_T and I_P are, respectively, the mass moments of inertia of the entire turbine and of the blade; M_i and M_{hi} are the instant torque produced by the single blade about turbine axis and about the blade hinge; M_C is the load torque; $\ddot{\alpha}$ is the blade pitch angle acceleration; $\ddot{\theta}$ is the turbine angular acceleration.
Any damping effects are not considered.

VORTEX METHODS: VAT-VOR3D CODE

Streamtube methods are able to correctly predict the turbine performances when rotor blades are not heavy loaded, and for Tip Speed Ratio (TSR = $\Omega R/V_\infty$) ,and solidity ($\sigma = N_b c_{hord}/R_{adius}$) values, not very high. For high values of TSR and σ such methods do not converge easily and are unreliable and inadequate. Part of these problems may be resolved with the use of the so-called "vortex models", which are based upon the vorticity equations. Such models allow a more realistic modeling of the flow field around and behind the turbine. The basic concept is to model the blade with a discrete number of lifting surfaces modeled by horseshoe vortex filaments: bound vortex and trailing vortex, Fig. 3. The production, convection and interaction of these vortex systems springing from the individual blade elements are used to predict the induced velocity at various points in the flow field.

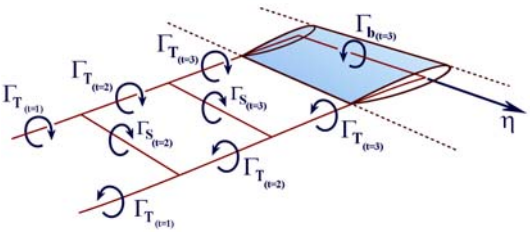

Fig. 3 – Unsteady vortex system of a blade segment

The bound vortex strength (Γ_b) is proportional to the lift acting on the blade segment by the Kutta-Joukowski law. The trailing vortex strength (Γ_T) is related to the change in bound vortex

strength along the blade span. During the blade revolution the local bound vortex strength changes with time, and, according to the Kelvin's theorem, a spanwise vortex is shed whose strength (Γ_S) is related to the rate of change of the bound vortex strength. These vortex systems (*B*ound, *T*railing, and *S*panwise) induce velocities on different points evaluated by the classic Biot-Savart law, from which the effective angle of attack is obtained and, consequently, the hydrodynamic forces acting on the blades are determined. The evaluation of the strength of the vortices and the local angle of attack on every blade segment requires an iterative procedure until converged values (of the bound system) are obtained. This model, differently from DMS, automatically takes into account the three dimensional effects. Strickland first proposed this method and developed the VDART3D code (Strickland, Webster and Nguyen, 1980) able to predict only Darrieus turbine performances. In order to investigate the hydrodynamic behaviour of the straight blade vertical axis turbines, with fixed and floating blades, the VAT-VOR3D code has been developed. In the figure below, Fig. 4, the numerical simulation, by VAT-VOR3D code, of the wake of a three blades turbine is presented. The continuous line connects the wake points shed by a single blade.

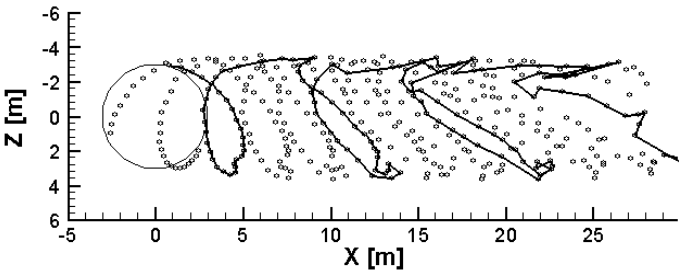

Fig. 4 - Numerical simulation of the wake for TSR=2 and σ=0.4

VAT-VOR3D numerical results have been compared with wake visualizations obtained with water tank tests at Sandia National Laboratories, Fig. 5.

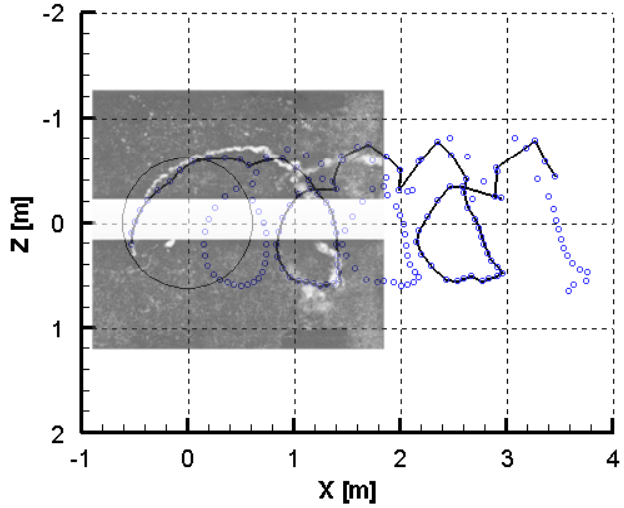

Fig. 5 - Comparison between numerical simulation, by VAT-VOR3D code, and experimental results (by Strickland, Webster and Nguyen, 1980). TSR = 2.5

To demonstrate the higher capability of the vortex model compared to the DMS model in the operating conditions characterized by high solidity, some comparisons between VAWT code and VAT-VOR3D code results have been made and presented below.

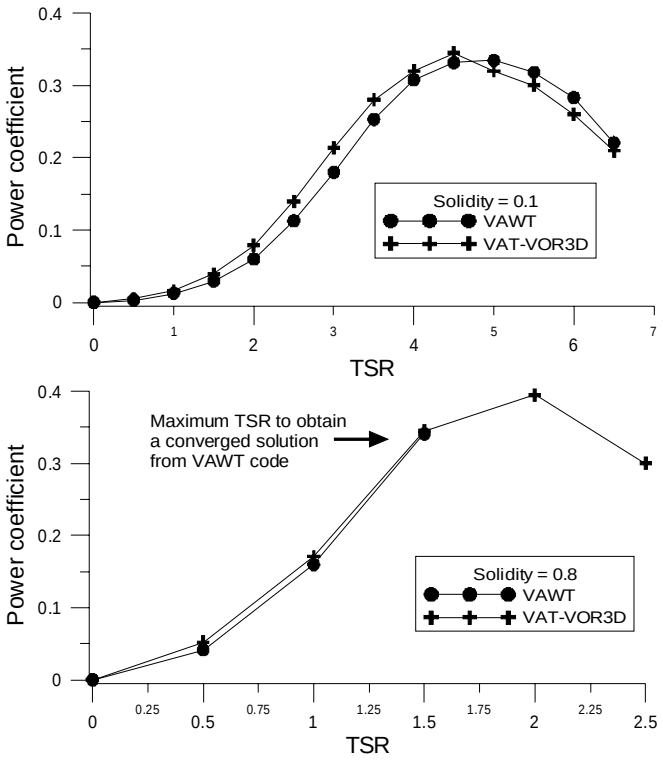

Fig. 6 - Comparison between vortex model and double multiple streamtube model for different solidity values

In graphs of Fig. 6, the limits of the DMS model are evident: over a certain TSR and solidity value, the VAWT code is not able to predict turbine performances.

USE OF VAT-VOR3D CODE TO INVESTIGATE THE INTERFERENCE BETWEEN TWO OR MORE TURBINES PLACED SIDE-BY-SIDE

The correct modeling of the interference between two or more turbines placed side-by-side, rotating in the same direction or counter rotating, Fig. 7, is very subtle because of the complexity of the physical phenomena involved and, at the same time, it is of the most importance in the optimal design of a plant with a number of turbines placed side-by-side.

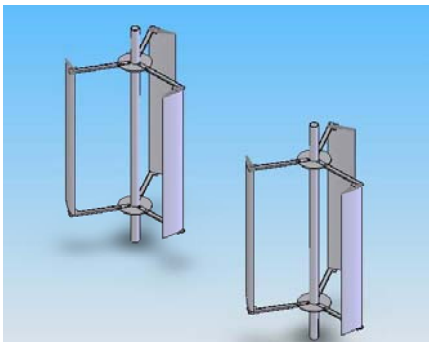

Fig. 7 - CAD representation of two turbines places side by side

In particular, it is important to determine the minimal inter-axial distance between the turbines to avoid significant interference effects and performance reduction. The knowledge of the minimal distance is fundamental to place the highest number of turbines in the site without reducing the hydrodynamic performances, or better, to maximize the annual energy that is possible to extract in that site. An extended version of the VAT-VOR3D code has been realized in order to evaluate these effects. Here, the preliminary numerical simulation of the wake structure behind two turbines placed side-by-side and rotating in the same direction is presented, Fig. 8. These aspects are still under evaluation.

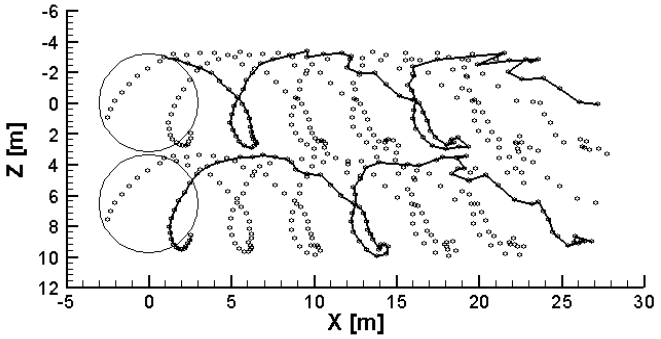

Fig. 8 - Numerical simulation of the wake behind turbines rotating in the same direction (solidity=0.4, TSR=1.5)

EXPERIMENTAL INVESTIGATIONS

The experimental data reported are divided in two parts: 1) experimental data measured in the DPA wind-tunnel on a small straight-bladed cycloturbine, which was designed, developed and assembled at DPA (Coiro and Nicolosi, 1998); 2) experimental data measured in water on the *KOBOLD* prototype (real scale) (Montella and Melone, 2003). Both the DPA straight-bladed cycloturbine (later on indicated also as Model A) and the *KOBOLD* prototype (later on indicated also as Model B) will be described as follow. Both turbines have variable pitch blades with a self-acting system, that is made up of two balancing mass for each blade. In this way, it is possible to move the blade gravity centre in its optimal position in order to optimize the global performance of the rotor and, using two stops, it is possible to limit pitch blade range, as shown in Fig. 9.

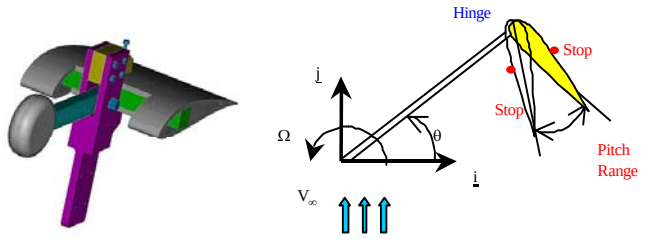

Fig. 9 Balancing Mass and Blade Stops

The model A in the DPA wind-tunnel is shown in the Fig. 10. Using different stop positions, it has been possible to test different pitch angle ranges, while using different number of blade it has been possible to take into account different solidity values.

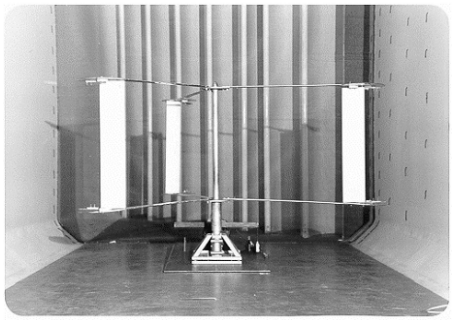

Fig. 10 - DPA straight-bladed cycloturbine (Model A)

The Model A has the following geometric parameters: number of blades tested 2, 3, 4, and 6; a blade chord of 0.15 m with a NACA 0018 airfoil; blade span 0.8 m length giving an Aspect Ratio of 5.33; radius of 1.05 m; $\sigma = 0.428$; two radial arms for each blade; arm chord of 0.05 m. The *KOBOLD* prototype (model B) lays out in the Strait of Messina (ITALY), close to the Sicilian shore. In this site the peak currents speed is 2 m/s (4 knots), the sea depth is 20 meters and the plant has been moored at 150 metres offshore. An high lift curved airfoil, called HLIFT18, is used for the blade sections and has been purposely designed at DPA to be cavitation free and to optimise the turbine performances. The use of a curved airfoil is one of the innovative aspects of this turbine. All existing vertical axis turbines employ symmetrical airfoils while it has been shown within this project that, with proper design, the curved airfoil works better than symmetrical ones (Montella and Melone, 2003). Two arms sustain each blade and the arms have been streamlined using another *ad hoc* designed symmetrical airfoil. Another innovative aspect of the *KOBOLD* turbine is the unique blade oscillation principle around hinge axis governed only by hydrodynamic and centrifugal forces. Thanks to this very simple way of oscillating, the turbine is able to start rotating autonomously showing high starting torque also with electrical load connected, without the necessity of any starting devices, and to speed up to the design angular rate, overcoming the typical starting difficulties of similar vertical axis turbines used in wind energy field (Darrieus, for example). The plant is composed by the turbine rotor hanging under a floating buoy that, in turns, contains the remaining mechanical and electrical parts needed to deliver energy to the electrical grid, see Fig. 11.

Fig. 11 - *KOBOLD* plant picture

The rotor has a diameter of 6 meters with 6 radial arms holding three blades with 5 meters span and with a chord of 0.4 m employing the HLIFT18 airfoil leading to an Aspect Ratio of 12.5 and to a solidity $\sigma = 0.4$. The acquisition data system is made up of a torque-meter, a tidal current speed-meter and a RPM counter all connected to a PLC that converts analog signals to digital data transferring them to a PC. A data handling software has been developed to monitor in real time the acquired data. The PLC acts also as electrical load controller to keep the turbine working always at its maximum efficiency independently from current speed. An international patent owned by *"Ponte di Archimede S.p.A"* company covers KOBOLD turbine project.

COMPARISON BETWEEN DMS NUMERICAL RESULTS AND EXPERIMENTAL DATA

VAWT and VAWT_DYN computer codes, based on the DMS theory, have been developed to predict the steady and dynamic performances of a cycloturbine with fixed or self-acting variable pitch straight-blades. These codes need of the 2D aerodynamic data. Regarding NACA airfoils, data are taken from literature (Paraschivoiu, 2002; Reuss, 1995), while for the HLIFT18 airfoil, TBVOR code (Coiro and de Nicola, 1989; Coiro, 1991) has been used to generate aerodynamic coefficients values. Airfoil 2D data are corrected, in VAWT and VAWT_dyn codes, to consider three-dimensional effects due to blade finite aspect ratio by mean Prandtl's lifting line theory. A 2D post-stall modelling, based on the Viterna-Corrigan correlation method (Eggleston and Stoddard, 1987), has been introduced to extend the 2D aerodynamic coefficients to these angle ranges (Montella and Melone, 2003). Moreover, arm losses have been included. In Figure 12, the comparison between VAWT code numerical results and experimental data measured on Model A with three blades, are shown. The power measured is the net rotor power and the tests are carried out with 9 m/s air speed in the DPA wind tunnel.

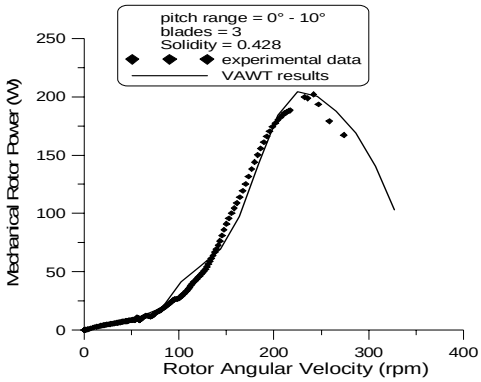

Fig. 12 - Experimental data and VAWT results (Model A)

Figure 13 shows the comparison between the experimental data, measured during field tests in water for the *KOBOLD* turbine prototype, and the VAWT code numerical prediction. The net rotor power coefficient is measured and the tests are carried out with a presumed current speed of 1.5 m/s, but there is an uncertainty around 25% on the real "undisturbed" current speed value that is strongly influenced by the location of the current speed-meter: this is currently being investigating. The net max rotor power coefficient is around 25 percent.

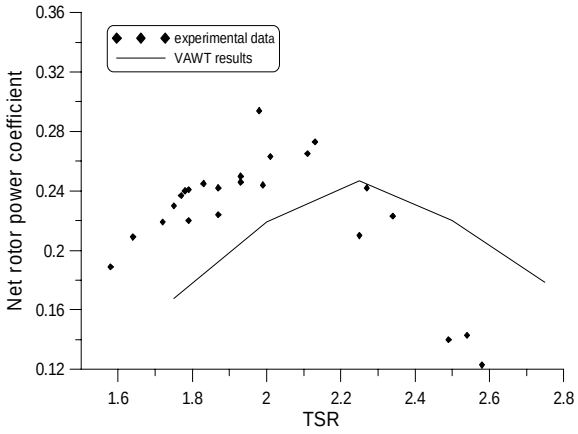

Fig. 13 - Experimental data and VAWT results (*KOBOLD*)

In Figure 14 are shown experimental data and VAWT_DYN code numerical results referred to the starting condition for the *KOBOLD* turbine prototype.

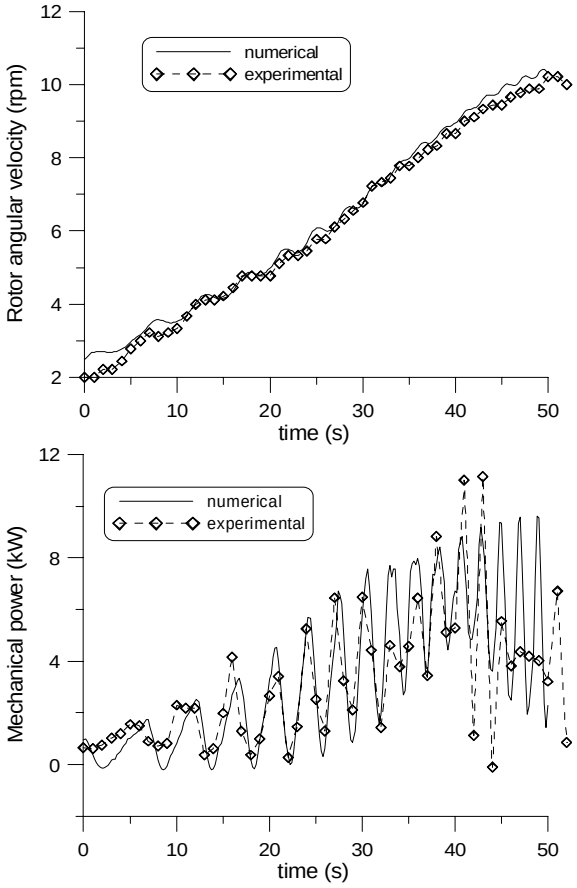

Fig. 14 - Experimental data and VAWT_DYN results (*KOBOLD*)

The time variation of the rotor angular velocity predicted by the code seems to be very accurate, while the rotor torque and power amplitudes are in a good agreement only in the first part of the time range: this is probably due to the uncertain value of the numerical predicted losses. The frequency of the torque and power are instead very well predicted.

FLOW CURVATURE EFFECTS

During our early investigations into the HLIFT18 performances using the Double Multiple Streamtube model (Montella and Melone, 2003), it was pointed out that turbine performances were too high; in fact, Cp maximum value was very close to Newman limit of 0.64 (Paraschivoiu, 2002). Making a comparison between the HLIFT18 and symmetrical airfoils performances, it was found that the airfoil momentum coefficient at ¼ of chord ($Cm_{1/4c}$) was the most important contribution to the difference in turbine torque and Cp values. It was also noted that in almost all previous numerical models the $Cm_{1/4c}$ contribution to the torque had been neglected. To evaluate if this contribution was necessary, an intensive analysis of actual flow on a vertical axis turbine blade was carried out and it was found that in all momentum models (Paraschivoiu, 2002; Strickland, 1986; Templin, 1974) and in almost all numerical methods, it was assumed that the relative flow on a turbine blade was composed by two vectors: one parallel to the free stream flow and the other derived from the angular velocity. Thus in every position along the circular path, it is assumed that the undisturbed relative velocity $\underline{V}_R$ is straight and approaches the airfoil with an angle of attack, Fig.15.

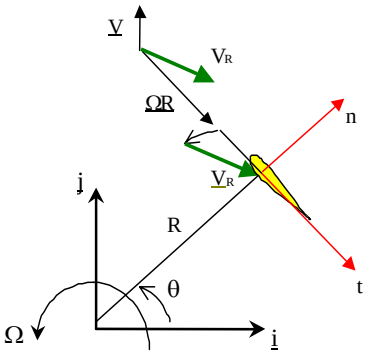

Fig. 15 - Typical relative flow on a blade in the DMS

This hypothesis is true only if the chord length is much smaller than the rotor radius (low solidity). In case of high solidity, because of the angular velocity of the rotor, the relative flow direction varies along the chord of a blade and at each point of the airfoil there is a different relative velocity (Hirsch, C. and Mandal, A.C. 1984). The result is that a symmetrical airfoil with zero pitch angle in a curved flow behaves like a curved airfoil with non-zero pitch angle in a straight flow, as it is shown in Fig. 16. Migliore et al. have investigated this for the first time in 1980 and they also performed some specific experiments to show this behaviour (Migliore, P.G., Wolfe, W.P. and Fanucci, J.B., 1980). This effect also depends on the ratio between the blade chord and rotor radius, i.e. from the solidity, as it is shown in Fig. 17. All these aspects are very important to evaluate the right aerodynamic characteristics of vertical axis turbines. To analyse the effects of the curved path on the airfoil performances, a first model considering only the rotor angular velocity (no incoming stream) has been set up. In Figure 18 it is shown the typical velocity assumption that is not able to calculate the flow curvature effects: a symmetrical airfoil set at zero pitch (the angle between airfoil chord and local tangent direction $\underline{t}$ of circular path) and hinged at 0% chord would behave like the same airfoil considered in a straight flow at zero angle of attack (no lift).

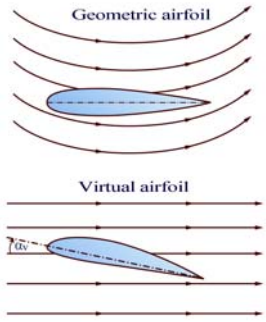

Fig. 16- Pictorial view of the flow curvature effect on a symmetrical airfoil

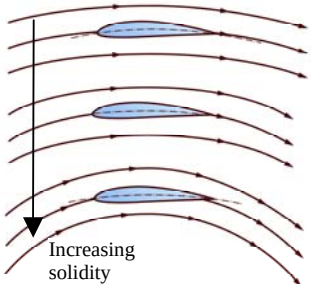

Fig. 17- Pictorial view of the flow curvature effect on a curved airfoil for different solidity values

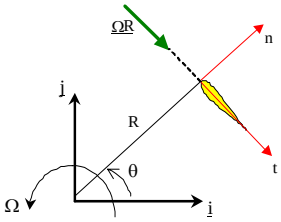

Fig. 18- Velocity scheme on a blade

To prove that this is not true, a numerical code, based on a 2D singularity panel method, able to simulate the inviscid aerodynamics of a generic airfoil in a curved flow, has been developed. The airfoil is represented by a number of panels on which singularities are distributed and the code solves the Laplace's equation for the velocity potential using a linear distribution of vortices on each panel (Coiro, 1991; Katz and Plotkin, 1991). The midpoint of each panel is a control point that "sees" a resulting velocity from the circular motion that is normal to the local radius, as it is shown in Fig. 19. The normal velocity component, V_n, is forced to be zero at the control point, this being the boundary condition on the surface. Summing the tangential component of the local velocity, V_t, with the velocity obtained from the solution of Laplace's equation, the final pressure distribution of an airfoil in pure curved flow is obtained.

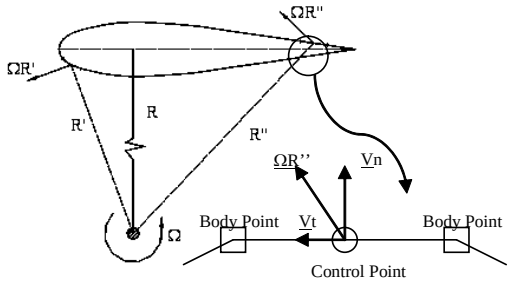

Fig. 19 - Qualitative scheme of velocities on different panels and single panel zoom

The airfoil's pressure coefficient, resulting from the code, obtained for a symmetrical airfoil in a curved flow with zero pitch and hinged at 0% chord, is very different from that expected from a symmetrical airfoil at zero angle of attack (i.e, no lift), see Fig. 20. It is important to note that the Cp bold-line

is referred to the lower surface of the airfoil: it shows a negative lift, indicating that the airfoil pressure coefficients correspond to an effective negative angle of attack.

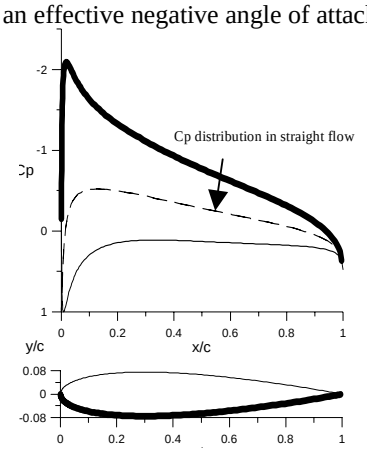

Fig. 20 - Pressure coefficient distribution: 2D panel method results

Some pressure distribution coefficients are shown in the following figure.

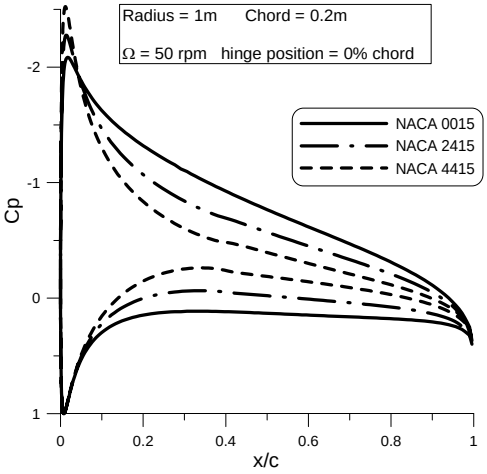

Fig. 21- Airfoil curvature effect on the pressure coefficient in a curved flow

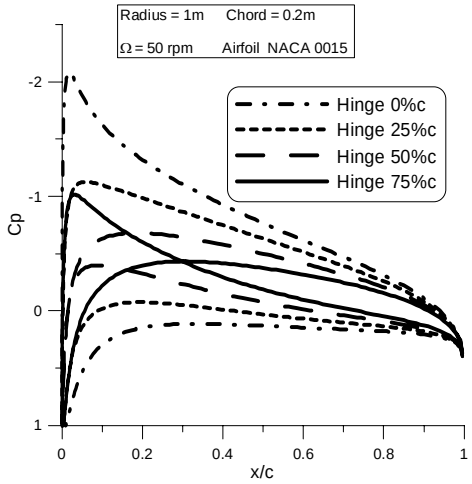

Fig. 22 – Hinge position effect on the pressure coefficient in a curved flow

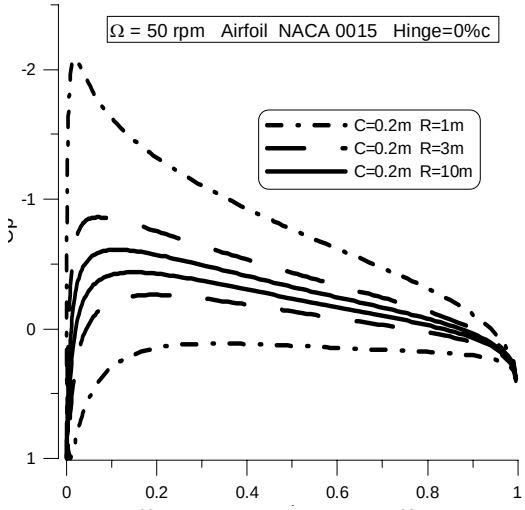

Fig. 23 - Solidity effect on the pressure coefficient in a curved flow

Figure 21 shows the Cp distributions relative to different airfoils characterized by same thickness but with increasing curvature: it can be clearly seen how the curvature effect diminishes as curvature increases. In Figure 22, the hinge position effect is reported while in Fig. 23 the solidity variation effect is shown. It is important to remind that in each Cp distribution the lower Cp values are on the lower airfoil surface, except for the airfoil hinged at 75% of chord. As already said it is important to point out that curvature effects become less important on a curved airfoil but it is also important to note that curvature effects become very small if the hinge is placed at 50% of chord length. Finally it can be inferred that the Cp distribution is very close to the no-lift condition if the solidity is low (Chord = 0.2m, Radius = 10m).

Further interesting aspects are the centre of pressure location and the aerodynamic forces direction in the case of a curved flow. It is important to note that viscous effects have not been taken into account in these calculations. As it can be seen in Fig. 24 independently from the center of pressure position, the resultant force always passes through the center rotation point and thus there is no contribution to the torque. If the viscosity had taken into account, the total aerodynamic force would have not passed through the rotation centre and would have created a braking moment.

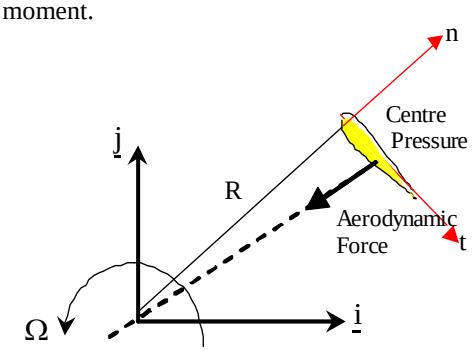

Fig. 24 - Aerodynamic force direction in no-viscous curved flow

In the Table 1 is reported the centre pressure position of three different airfoils in the same curved flow. Each airfoil is hinged

at 0% of chord and they have the same chord length. It is possible to see that the NACA 4415 airfoil has the centre of pressure closer to the hinge point than the others.

Radius = 1m Chord = 0,2 m Ω = 50 rpm Hinge = 0%c

Airfoil	Centre Pressure Position (x/c)
Naca 0015	0.33
Naca 2415	0.28
Naca 4415	0.19

Table 1 - Airfoil curvature effect on the centre of pressure position in a curved flow

In Table 2 it is shown the centre of pressure position for the NACA 0015 airfoil in the same curved flow with three different hinge point location. It is important to point out that the angle between the airfoil chord and turbine radius is always 90 degree.

Radius = 1m Chord = 0,2 m Ω = 50 rpm Airfoil 0015

Hinge Position	Centre Pressure Position (x/c)
Hinge 0%c	0.33
Hinge 25%c	0.28
Hinge 50%c	0.19

Table 2 - Hinge position effect on the centre of pressure position in curved flow

In Figure 25 the total aerodynamic force on the NACA 0015 airfoil in curved flow is shown considering three different hinge point positions. It is possible to see that the aerodynamic force is big if the hinge point is placed at 0% of chord and it gets smaller as the hinge point moves toward trailing edge. As already pointed out, the global force has no contribution to the moment respect to the turbine axis while there is a moment respect to the hinge point on the airfoil.

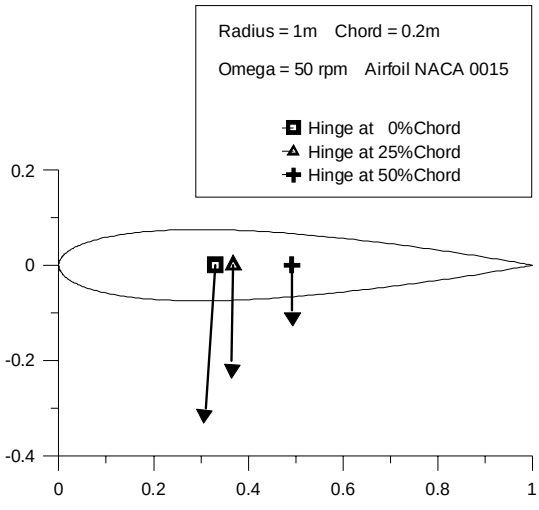

Fig. 25 – Hinge position effect on the aerodynamic force in curved flow

From these last considerations, it is possible to establish that the momentum coefficient respect ¼ of chord has to be taken into account in the turbine torque evaluation: if it had to be neglected, the aerodynamic force would be applied always at ¼ chord and would pass through the centre rotation point again. On the contrary, flow curvature effects have influence on the actual value of aerodynamic coefficients. This could explain why using the Double Multiple Streamtube model with strong cambered airfoil the turbine performances are too high: the real moment coefficient of airfoil in curved flow could be much smaller. The last aspect of the investigation about flow curvature effect on airfoils concerns the possibility of designing a new airfoil shape to avoid detrimental aerodynamic changes and to improve the turbine performances. Evaluating the velocities in each control point of the airfoil in a curved flow, it is possible to use them in a design code. Such code has been developed in the past at DPA and it is capable to give an airfoil shape once the velocities in the corners points are assigned. In Figure 26 it is shown the Curved Flow Airfoil that has been obtained starting from a NACA 0015 imposing the same velocities that NACA0015 presents when it is set in a curved flow. The angle of attack has been imposed equal to 5 degrees.

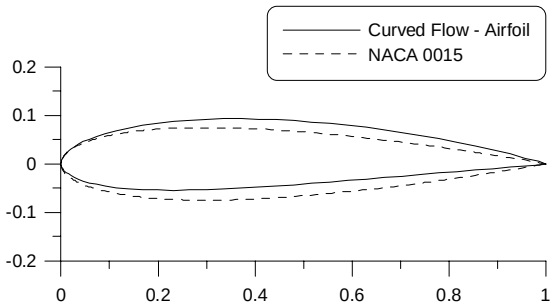

Fig. 26 – New airfoil shape able to work in curved flow conditions

Using the curved flow-panel method previously described, the pressure coefficient distribution reported in Fig. 27 has been obtained. It can be clearly seen that the Cp distribution for the new airfoil set in a curved flow is exactly the same of the NACA 0015 airfoil set in a straight flow at zero angle of attack. In the same picture it is also shown the Cp distribution used as target for the design code and that is the same that NACA 0015 would have if it had set in curved flow.

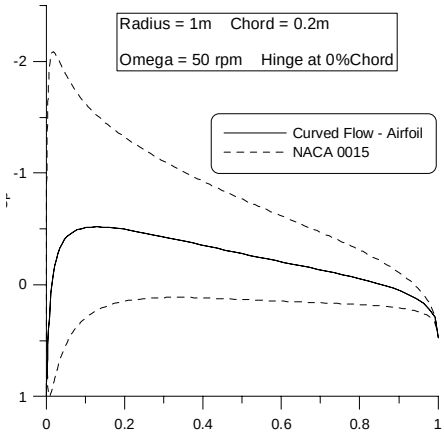

Fig. 27 – Cp distributions of the NACA 0015 and the Curved – Flow Airfoil in a curved flow

At present, several other aspects about the best airfoil shape to improve the turbine performance are under investigation. For example it is important to evaluate the airfoil contribution to the turbine torque both in upwind and downwind sites and to choose in which side it would be better to optimize the airfoil shape.

CONCLUSIONS

The Double Multiple Streamtube model seems to be good in predicting of the vertical axis turbine performances especially for solidity values less than 0.5. This model has been implemented in VAWT and VAWT_dyn codes that are then capable of predicting both static and dynamic performances of the turbine with very low computing time. In these codes blade 3D effects have been included as well as arm losses, while it is difficult to predict the losses due to other effects. In the field tests, the accuracy of the tidal speed current measurement is a problem, because it is difficult to set the current speed-meter in the "real" undisturbed flow, so the measurements have an uncertainty level around the 25%. To overcome typical problems of the DMS model, VAT-VOR3D code, based on a vortex method, has been developed. For low solidity values VAWT and VAT-VOR3D results are very close. For higher solidity values, VAWT code break down, because it does not converge, while VAT-VOR3D code is able to evaluate more accurately turbine performances but with a very long computational time. The code, opportunely modified, is also able to simulate the interference of two, or more, turbines places side-by-side, counter rotating or rotating in the same verse. This aspect, still under investigation, is very important in order to evaluate the correct inter-axial distance between them, avoiding stronger interference effects and performances reduction. Flow curvature effects on vertical axis turbine blade are evaluated by a 2D panel method. This numerical analysis points out that airfoils in curvilinear flow exhibit aerodynamic characteristics very different from what they would in rectilinear flow, especially when the solidity is high. Hinge position effects on airfoil's Cp distributions in curved flow have been highlighted. The influence of the solidity and of the airfoil curvature effect has been also investigated. It has been noted that curvature effects become less important on a curved airfoil. Moving the hinge position, flow curvature effects become very small if the hinge is placed at 50% of chord length. Another important result regards the aerodynamic force direction: the curved flow code has shown that it always passes through the centre of rotor's rotation. Finally, an airfoil design code has been used to design a shape able to eliminate the aerodynamic effects due to the curved flow. Further investigations are necessary to achieve the best airfoil shape that is able to maximize the whole turbine performances.

REFERENCES

Coiro, D.P. and Nicolosi, F. (1998). "Numerical and Experimental Tests for the KOBOLD Turbine," SINERGY Symposium, Hangzhou, Republic of China.

Coiro, D.P. and de Nicola, C. (1989). "Prediction of Aerodynamic Performance of Airfoils in Low Reynolds Number Flows," Low Reynolds Number Aerodynamics Conference, NotreDame, Indiana, U.S.A..

Coiro, D.P. and de Nicola, C. (1989). "Low Reynolds Number Flows: The Role of the Transition," X Congresso Nazionale AIDAA, Pisa.

Coiro, D.P. (1991). "Convergence Acceleration Procedure for a Viscous/Inviscid Coupling Approach for Airfoil Performances Prediction," XI AIDAA National Congress, Forlì, Italy.

Eggleston, D.M. and Stoddard, F.S., (1987). "Wind Turbine Engineering Design," Van Nostrand Reinhold Company, New York.

Hirsch, C. and Mandal, A.C. (1984). "Flow Curvature Effect on Vertical Axis Darrieus Wind Turbine Having High Chord-Radius Ratio," European Wind Energy Conference, Hamburg, Germany.

Katz, J., Plotkin, A. (1991). Low Speed Aerodynamics – from Wing Theory to Panel Methods, McGraw-Hill International Editions – Aerospace Science Series.

Kentfield, J.A.C. (1983). "Cycloturbines with freely hinged blades or freely hinged leading edge slats," Alternative Energy Sources V. Part C: Indirect Solar/Geothermal, (Editor: T.N. Veziroglu). Amsterdam: Elsevier Science Publishers B.V., p. 71-86.

Kirke, B.K. and Lazauskas, L. (1993). "Experimental Verification of a Mathematical Model for Predicting the Performance of a Self-Acting Variable Pitch Vertical Axis Wind Turbine," WIND ENGINEERING, 17 (2), p. 58-66.

Lazauskas, L. (1992). "Three Pitch Control Systems for Vertical Axis Wind Turbines Compared," WIND ENGINEERING, 16 (5), p. 269-281.

Migliore, P.G., Wolfe, W.P. and Fanucci, J.B. (1980). "Flow Curvature Effects on Darrieus Turbine Blade Aerodynamics," Journal of Energy, 4 (2), p. 49-55.

Montella, F. and Melone, S. (2003). "Analisi Sperimentale e Numerica del Comportamento Statico e Dinamico di una Cicloturbina ad Asse Verticale," Aerospace Engineering Bachelor Thesis. Università di Napoli Federico II, Dipartimento di Progettazione Aeronautica, Italy.

Paraschivoiu, I. (2002). Wind Turbine Design with Emphasis on Darreius Concept, Ecole Polytechnique de Montreal, Polytechnic International Press.

Reuss, R.L. et al. (1995). "Effects of Surface Roughness and Vortex Generators on the NACA 4415 Airfoil," Report: NREL/TP-442-6472. Golden, Colorado: National Renewable Energy Laboratory.

Strickland, J.H. (1986). "A review of aerodynamic analysis methods for vertical-axis wind turbine," Fifth ASME Wind Energy Symposium, SED-Vol.2 edited by A.H.P. Swift.

Strickland, J.H., Webster, B.T. and Nguyen T. (1980). "A vortex Model of the Darrieus Turbine: an Analytical and Experimental Study," SAND79-7058 Contractor Report.

Templin, R.J. (1974). "Aerodynamic Performance Theory for the NCR Vertical Axis Wind Turbine," Report: LTR-LA-160. National Research Council of Canada.

Zhang, L., Wang, L. and Li, F. (2004). "Study on streamtube models for prediction of performance of vertical-axis variable-pitch turbine for tidal current energy conversion," Journal of Harbin Engineering University, 25 (3), p. 1-10.